MECHANISMS OF DEVELOPMENT 125 (2008) 797–808

available at www.sciencedirect.com

ScienceDirect

journal homepage: www.elsevier.com/locate/modo

MECHANISMS OF DEVELOPMENT

Cell lineage in mammalian craniofacial mesenchyme

Toshiyuki Yoshida[a], *Philaiporn Vivatbutsiri*[a], *Gillian Morriss-Kay*[b], *Yumiko Saga*[c], *Sachiko Iseki*[a,*]

[a]*Department of Molecular Craniofacial Embryology, Graduate School, Tokyo Medical and Dental University, 1-5-45 Yushima, Bunkyo-ku, Tokyo 113-8549, Japan*
[b]*Department of Physiology, Anatomy and Genetics, Le Gros Clark Building, South Parks Road, Oxford OX1 3QX, UK*
[c]*Division of Mammalian Development, National Institute of Genetics, and Department of Genetics, Sokendai, Yata 1111, Mishima, Shizuoka 411-8540, Japan*

ARTICLE INFO

Article history:
Received 27 February 2008
Received in revised form
14 May 2008
Accepted 13 June 2008
Available online 20 June 2008

Keywords:
Mesoderm
Neural crest
Mesp1-cre
Wnt1-cre
Tissue boundary
Skull

ABSTRACT

We have analysed the contributions of neural crest and mesoderm to mammalian craniofacial mesenchyme and its derivatives by cell lineage tracing experiments in mouse embryos, using the permanent genetic markers *Wnt1-cre* for neural crest and *Mesp1-cre* for mesoderm, combined with the *Rosa26* reporter. At the end of neural crest cell migration (E9.5) the two patterns are reciprocal, with a mutual boundary just posterior to the eye. Mesodermal cells expressing endothelial markers (angioblasts) are found not to respect this boundary; they are associated with the migrating neural crest from the 5-somite stage, and by E9.5 they form a pre-endothelial meshwork throughout the cranial mesenchyme. Mesodermal cells of the myogenic lineage also migrate with neural crest cells, as the branchial arches form. By E17.5 the neural crest-mesoderm boundary in the subectodermal mesenchyme becomes out of register with that of the underlying skeletogenic layer, which is between the frontal and parietal bones. At E13.5 the primordia of these bones lie basolateral to the brain, extending towards the vertex of the skull during the following 4–5 days. We used DiI labelling of the bone primordia in ex-utero E13.5 embryos to distinguish between two possibilities for the origin of the frontal and parietal bones: (1) recruitment from adjacent connective tissue or (2) proliferation of the original primordia. The results clearly demonstrated that the bone primordia extend vertically by intrinsic growth, without detectable recruitment of adjacent mesenchymal cells.

1. Introduction

Cell lineage tracing studies have made a major contribution to our understanding of the developmental architecture of the vertebrate head, and to the way in which juxtapositions between tissues of different origins may contribute to further development and growth. These studies have mainly relied on two approaches: externally applied tracers or inter-embryonic transplantation (mainly chick-quail chimaeras) (Le Douarin and Kalcheim, 1999, and references therein). In mammalian embryos (rat and mouse), extrinsic cell labelling and transplantation approaches to craniofacial development have been restricted by the time period during which the embryos are accessible in vitro (Tan and Morriss-Kay, 1986; Osumi-Yamashita et al., 1994; Trainor et al., 1994; Trainor and Tam, 1995), or by the duration of a label injected in vivo (Serbedzidja et al., 1992), so they have not yielded information on the relationship between tissue origins and fates. These

* *Corresponding author*. Tel.: +81 3 5803 5579; fax: +81 3 5803 5578.
E-mail address: s.iseki.emb@tmd.ac.jp (S. Iseki).
0925-4773/$ - see front matter
doi:10.1016/j.mod.2008.06.007

limitations were recently overcome by the use of a permanent molecular marker for neural crest cells, created by mating mice carrying the *Wnt1-cre* construct with mice carrying the *Rosa26* reporter gene in all cells (Jiang et al., 2000). In all mice carrying both constructs (*Wnt1-cre/R26R*), from neural crest cell migration stage embryos to adults, *LacZ* is expressed in all cells that have ever expressed *Wnt1,* i.e. in cells originating in part of the cranial neural plate, the dorsal neural tube and in all of the neural crest (Danielian et al., 1998). Hence X-gal staining has enabled neural crest cells and their derivatives to be distinguished from cells of mesodermal origin in the developing cardiovascular system and head, including the skull vault (Jiang et al., 2000, 2002; Chai et al., 2000).

At the time of our original skull vault lineage study (Jiang et al., 2002), we did not have access to a transgenic mouse with a permanent cell marker for mesoderm, and we were only able to detect mesoderm-derived cells through their failure to stain with X-gal and through a short-term DiI labelling study. Major boundary sites between neural crest and mesoderm such as the coronal (fronto-parietal) suture were clearly distinguishable, but subtle cell mixing involving a small number of mesoderm-derived cells within an apparently homogeneous neural crest-derived mesenchymal compartment could not be detected. Here we introduce a transgenic mouse, *Mesp1-cre/R26R*, in which mesoderm is specifically and permanently labeled, enabling embryonic cranial mesenchymal cells of mesodermal origin to be distinguished from those derived from neural crest within a mixed population. *Mesp1*, a basic helix–loop–helix transcription factor, was first cloned by subtraction of expressed RNA between anterior and posterior part of the bodies of E7.5 embryos (Saga et al., 1996). Its expression is first observed at E6.5 (early gastrulation stage), specifically in the nascent mesodermal cells including extra-embryonic mesoderm; it is down-regulated shortly after the end of gastrulation, the last expression being in presomitic mesoderm around E9.5. In order to follow the mesodermal cell lineage, *cre*-recombinase was introduced into the genome under the control of endogenous *Mesp1* promoter and the expression was monitored using *CAG-CAT-Z* reporter mice (Sakai and Miyazaki, 1997). Analysis of the resulting embryos revealed the mesodermal contribution to the heart primordium (Saga et al., 1999). However, the contribution of *Mesp1*-lineages other than heart primordia have not been investigated systematically although it is expected to contribute the major part of all endothelial cell lineages including yolk sac vasculature.

In this study we have investigated distribution of *Mesp1*-lineage cells using *Mesp1-cre* and *R26R* mice to further define the mesoderm-derived tissue in the developing head. The results confirm the mesodermal contributions to the skull vault assumed from the X-gal-negative results in the earlier *Wnt1-cre/R26R* neural crest detection study (Jiang et al., 2002). They additionally reveal the presence of small numbers of mesodermal cells within the neural crest-derived frontonasal mesenchyme, beginning at very early neural crest cell migration stages. Co-localisation of these X-gal-positive cells with endothelial and muscle cell lineage markers revealed the timing of migration of pre-endothelial and pre-muscle cells into the neural crest-derived mesenchyme, and their positions.

In addition to the mesodermal cell lineage study, we have further investigated the process of skull vault growth by DiI labeling of the frontal and parietal bone primordia in ex-utero embryos and allowing development to continue in vivo.

2. Results

2.1. *Cranial mesoderm expresses LacZ in the Mesp1-cre/R26R mouse*

Mesp1 is expressed in primary mesenchyme, the earliest group of cells ingressing upon gastrulation, and all mesodermal derivatives in the yolk sac (Saga et al., 1999). Its expression was therefore expected in the cranial mesenchyme that is present prior to the start of neural crest cell migration. In 5-somite stage (E8.5) *Mesp1-cre/R26R* embryos, the cranial mesenchyme is indeed X-gal-positive, except for a small number of cells adjacent to the neuroepithelium and surface ectoderm of the diencephalon/midbrain/rostral hindbrain regions (Fig. 1A and B and data not shown). These cells are identified as recently emigrated neural crest by X-gal staining of *Wnt1-cre/R26R* embryos and by their more rounded morphology (Fig. 1C and D). *Wnt1* is expressed in the neuroepithelium of the diencephalon, midbrain and rostral hindbrain (Parr et al., 1993; Echelard et al., 1994); correspondingly, *LacZ* is expressed in these areas of the neuroepithelium in *Wnt1-cre/R26R* embryos, as previously reported (Jiang et al., 2002). The heart primordium of *Mesp1-cre/R26R* embryos is X-gal-positive, consistent with previous data (Fig. 1A and Saga et al., 1999).

At the 5-somite stage, the basement membrane of the rostral forebrain neuroepithelium is closely apposed to that of the surface ectoderm. It is not until after the onset of neural crest cell migration into this rapidly growing region that the two basement membranes separate and neural crest cells migrate between them, as seen at the 8-somite stage (Fig. 1G and Jiang et al., 2002). X-gal staining of *Mesp1-cre/R26R* embryos revealed that mesodermal cells migrate into this potential space at the same time as the neural crest cells (Fig. 1E). Comparison of sections through the midbrain neural fold and nascent first arch of *Mesp1-cre/R26R* and *Wnt1-cre/R26R* embryos suggest that although the main neural crest cell pathway is subectodermal, as previously reported (Nichols, 1981; Chan and Tam, 1988) and illustrated in Fig. 1F, the staining patterns suggest that there is considerable mixing of the two cell types (compare Fig. 1F and H).

2.2. *Mesoderm localization after neural crest migration*

X-gal staining of *Wnt1-cre/R26R* embryos suggests that by E9.5, neural crest cell migration into the frontonasal region, first arch and trigeminal ganglion is complete, with a clear boundary between the neural crest-derived and non-crest mesenchyme (Jiang et al., 2002 and Fig. 2A). In contrast, the staining pattern of whole *Mesp1-cre/R26R* heads shows a reticular pattern covering the entire cranial neural tube and extending into the branchial arches (Fig. 2B), resembling the pattern of CD34 expression in embryonic blood vessels at this stage (Wood et al., 1997). In addition to the reticular staining pattern there is more solid staining seen where most of the

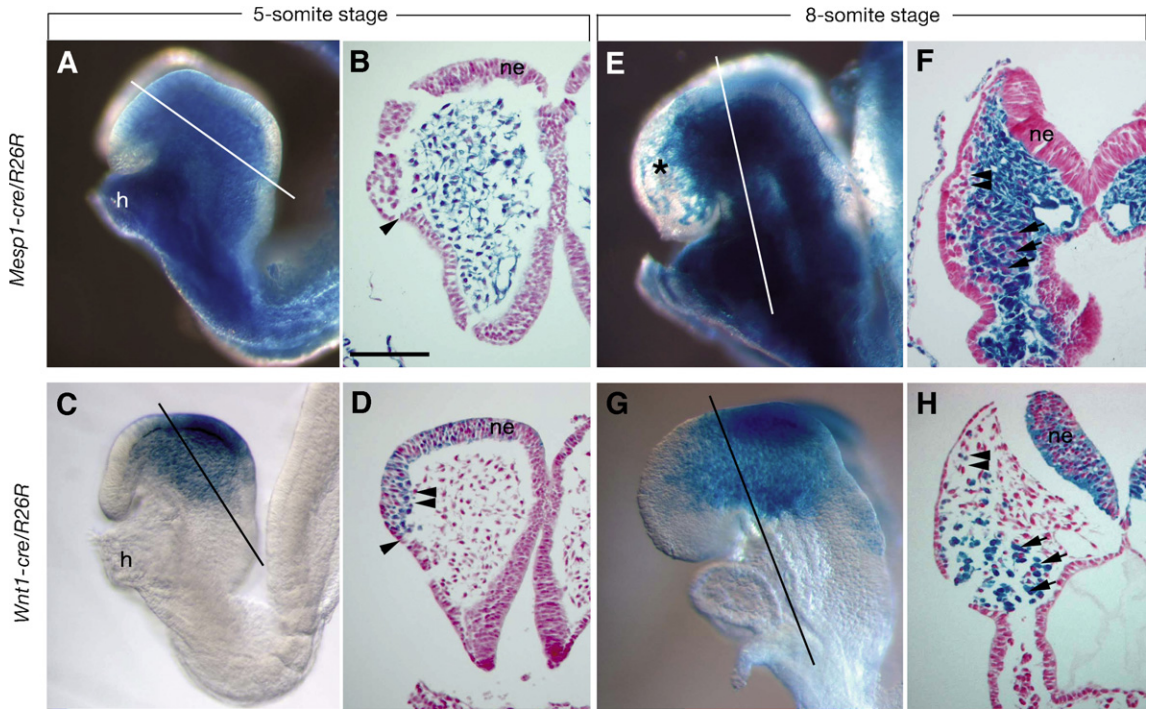

Fig. 1 – Craniofacial mesenchyme: mesoderm and neural crest cell origins at 5- and 8-somite-stages in *Mesp1-cre/R26R* and *Wnt1-cre/R26R* embryonic heads as indicated, stained with X-gal. Orientation of the sections is indicated by lines on the whole heads. (A, B) At the start of neural crest cell migration, cranial mesenchyme, including the heart primordium (h), is of mesodermal origin. Neuroepithelium (ne) and ectoderm (the boundary is indicated by an arrowhead) are X-gal-negative. (C, D) Neural crest cells (double arrowheads in D) have just begun to migrate and are the only X-gal-positive mesenchyme cells; midbrain and rostral hindbrain neuroepithelium is also X-gal-positive. E and F show a slightly less advanced 8-somite-stage embryo than G and H, on the basis of forebrain shape. (E) As mesodermal mesenchyme extends between the separating basement membranes of the neuroepithelium and surface ectoderm, the stained cells form a reticular pattern among X-gal-negative cells (asterisk). (F) Unstained migrating neural crest cells are mainly in the subectodermal pathway (double arrowheads). (G, H) In addition to formation of frontonasal mesenchyme, neural crest cells are migrating ventrally, mixed with mesoderm-derived mesenchyme (arrows). X-gal staining of the sections shown in F and H is mutually exclusive. Scale bar: B, D, F, H 100 μm.

thickness of the embryo is made up of mesenchyme, i.e. within and adjacent to the embryonic axis (Fig. 2B, white dotted line). Horizontal sections through the forebrain and rostral hindbrain show that although the neural crest respects the mesenchymal boundary adjacent to the diencephalon (Fig. 2C and D), the mesodermal mesenchyme does not (Fig. 2G and H). Some of the mesodermal cells within the mainly neural crest-derived frontonasal mesenchyme can be seen to be the endothelium of blood vessels (arrowheads, Fig. 2H). The blood vessels contain X-gal-stained blood cells; these are derived from the yolk sac mesoderm at this stage (Wood et al., 1997 and references therein). The solid mesodermal staining extends from the axial mesoderm into the branchial arches as a core of X-gal-positive cells within the reticular meshwork (Fig. 2B, asterisks). Coronal sections through the midbrain and first branchial arches of embryos of both genotypes confirm that the core of the arch is mesodermal (Fig. 2F and J). These sections also reveal more scattered mesodermal cells among the more peripheral neural crest-derived mesenchyme (this is clearer in the *Mesp1-cre/R26R* sections, since the blue stain stands out more clearly against the pink than vice versa). Sections through the first and second branchial arches show that the mesodermal core is situated lateral to the aortic arch arteries (Fig. 2K). The endothelial walls of the arch arteries were, as expected, mainly stained by X-gal in the *Mesp1-cre/R26R* (Fig. 2K). Fig. 2L shows a parallel but more dorsal plane, in which the mesenchyme is almost entirely mesodermal, as are the walls of the cardinal veins.

The X-gal staining pattern of whole *Mesp1-cre/R26R* heads at E10.5 is the reciprocal of that reported for *Wnt1-cre/R26R* embryos (Jiang et al., 2002), except for the reticular pattern in the mainly neural crest area and a dense blue core in the branchial arches (Fig. 2M). At this stage the density of the staining obscures the reticular pattern observed around the neural tube at E9.5.

2.3. *Endothelial lineage of cranial mesoderm*

The X-gal staining patterns for *Mesp1-cre/R26R* embryos from E8.5 to E10.5 suggest that mesodermal cells of both endothelial and myogenic lineages mingle with neural crest cells from early stages of neural crest cell migration. To test this hypothesis with respect to the endothelial

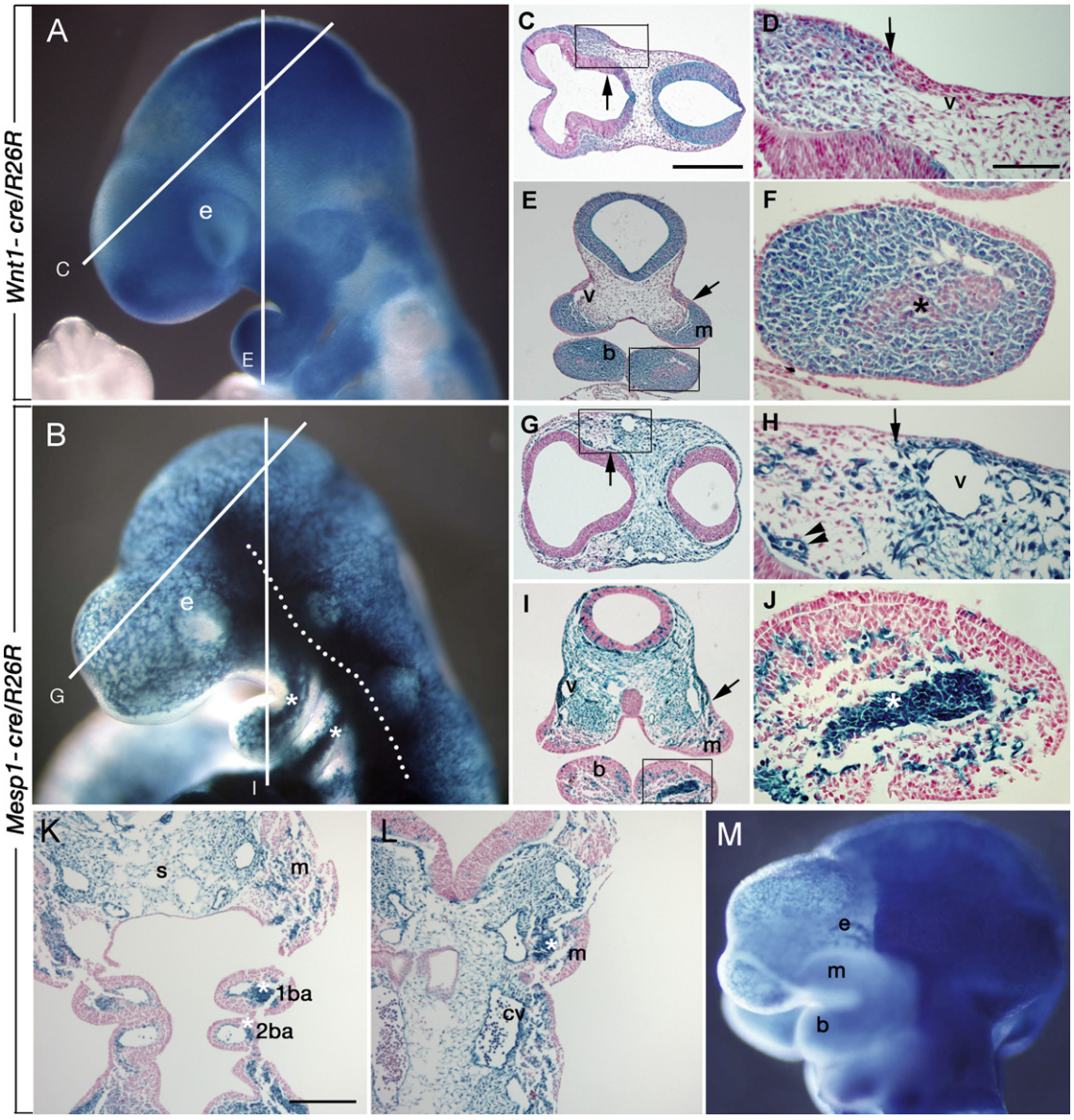

Fig. 2 – The rostral boundary between neural crest and mesoderm forms after neural crest migration: X-gal staining of *Wnt1-cre/R26R* (A, C–F) and *Mesp1-cre/R26R* (B, G–M) embryos; (A–L) E10.0, (M) E10.5. White lines in A and B indicate planes of adjacent sections; D,F,H and J are magnified images of the boxes in C,E,G and I. Arrows indicate the boundary between neural crest- and mesoderm-derived mesenchyme. (A) After neural crest cell migration, neural crest cells comprise the mesenchyme rostral to and around the eye, the maxillary and mandibular swellings and the trigeminal ganglion anlagen. Mid- and hindbrain neural tube is also stained. (B) *Mesp1-cre*-positive mesoderm is observed in a reticular pattern coinciding with *Wnt1-cre*-positive and -negative areas; dense staining is present ventral to the neural tube along the embryonic axis (white dotted line) and extends into the core of each branchial arch (asterisks). (C, D) A horizontal section shows that the neural crest-mesoderm boundary (arrow) in the head mesenchyme lies adjacent to the diencephalon. (E) In the maxillary process, the boundary (arrow) is at the proximal edge of the maxillary prominence (m); mandibular mesenchyme mostly comprises neural crest cells (b). (F) There is an X-gal-negative mesodermal core (asterisk) in the center of the mandibular mesenchyme. (G–J) The mesenchymal staining pattern of *Mesp1-cre/R26R* sections is reciprocal to that of *Wnt1-cre/R26R* sections except that scattered mesodermal cells are present within the mainly neural crest-derived mesenchyme; some of these form blood vessels and blood cells (double arrowheads in H). (K, L) Frontal sections through the first and second branchial arches (K) and just dorsal to that position: mesenchyme under the neural tube is derived from mesoderm and flanked by mainly neural crest derived maxillary processes (m); mesodermal cores (white asterisks) in the first (1ba) and the second (2ba) branchial arches are present lateral to the aortic arch arteries, which are composed of mesoderm-derived endothelial cells. (M) Whole mount X-gal staining of an E10.5 *Mesp1-cre/R26R* head reveals a clear mesodermal boundary reciprocal to that of *Wnt1-cre/R26R* specimens (see Jiang et al., 2002 for a more comparable stage). cv, anterior cardinal vein; e, eye; v, major blood vessels. Scale bars: C, E, G, I 200 μm; D, F, H, J 100 μm; K and L 200μm.

lineage, we used immunohistochemistry to detect two endothelial lineage markers, CD31 and Flk1. CD31 gave a poor result at neural crest cell migration stages (not shown). Flk1 expression is widespread within the head mesenchyme at the onset of neural crest cell migration (Fig. 3A), the area in which frontonasal neural crest cells are migrating (Fig. 3B). Immunohistochemical detection of Flk1 on sections of X-gal-stained *Wnt1-cre/R26R* embryos shows Flk1-positive/X-gal-negative cells scatter within the neural crest cell population (Fig. 3C), indicating that mesodermal cells of the endothelial lineage migrate with neural crest cells.

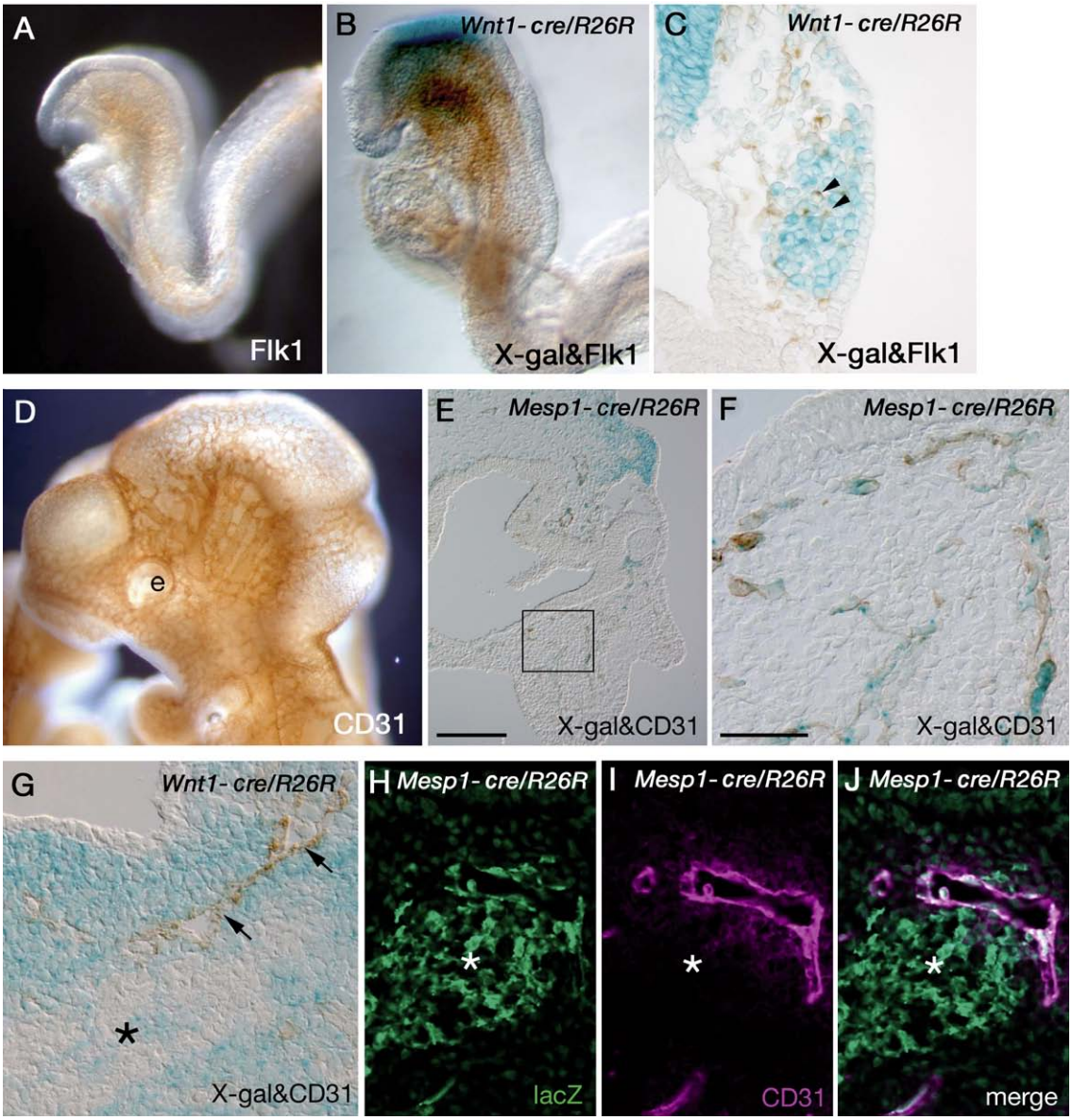

Fig. 3 – Localization of endothelial cell lineage. (A) Whole mount immunohistochemical detection of Flk1 on E8.5 (5-somite stage) wild type embryo. Flk1 is found in the most of the rostral mesenchyme. (B) X-gal staining and Flk1 immunohistochemical detection on *Wnt1-cre/R26R* E8.5 (11-somite stage) embryo. (C) Frontal section of a *Wnt1-cre/R26R* E8.5 specimen (11-somite stage) after whole mount X-gal staining and immunodetection of Flk1. Some Flk1-positive/X-gal-negative cells (arrowheads) are present among the X-gal-positive neural crest cells. (D) Immunohistochemical staining of PECAM (CD31) of a wild type E10.5 embryo. (E) X-gal staining and CD31 immunohistochemistry on a horizontal section of the nasal area of an E10.5 *Mesp1-cre/R26R* embryo. (F) A magnified image of the boxed area in E, showing X-gal-positive/CD31-positive endothelial cells. (G) X-gal staining and immunohistochemistry of CD31 on a horizontal section of E10.5 *Wnt1-cre/R26R* first branchial region. Arrows indicate CD31-positive and X-gal-negative endothelium adjacent to pharynx. The mandibular mesenchyme contains both neural crest and mesodermal cells. (H–J) Double immunofluorescent detection of lacZ (H), CD31 (I) and their superimposed image (J) in the mesodermal core (asterisks) of the first branchial arch of an E10.5 *Mesp1-cre/R26R* embryo. The mesodermal core (asterisk) is lacZ-positive (H); blood vessels are present in the periphery of the core (I) but the major mesodermal component comprises non-endothelial lineage cells. e, eye. Scale bars: C, F–J 50 μm; E 200 μm.

The pattern of immunohistochemical staining with CD31 on a whole head at E10.5 is illustrated in Fig. 3D: the distribution of developing blood vessels within the cranial mesenchyme is evenly spread across the areas populated principally by cells of either neural crest or mesodermal origin (Compare with Fig. 2M). This is confirmed by combining X-gal staining and immunohistochemistry on sections of embryos of both genotypes. In the frontonasal mesenchyme of *Mesp1-cre/R26R* embryos, all of the immunostained cells are X-gal-positive (Fig. 3E and F); in contrast, *Wnt1-cre/R26R* embryos show mutually exclusive CD31 immunostaining and X-gal staining (Fig. 3G). Double immunofluorescence detection of LacZ and CD31 in *Mesp1-cre/R26R* embryos shows that in the branchial arches, CD31 is expressed in the X-gal-positive endothelium of small blood vessels but not in the X-gal-positive core mesenchyme of the mandibular arch (Fig. 3H–J), indicating that only a part of *Mesp1*-lineage differentiates to endothelial cells in the mandibular arch. In other word, cells expressing *Mesp1* are composed of at least two distinct cell populations, endothelial cells and non-endothelial mesenchymal cells, possibly myogenic.

2.4. *Localization of myogenic cell lineage mesoderm*

To test the hypothesis that the X-gal-positive core mesenchyme of the branchial arches of E9.5 *Mesp1-cre/R26R* embryos (Fig. 2B asterisk) is myogenic, we carried out X-gal staining and in situ hybridization for *MyoD* on the same section (Fig. 4A). The sections show that the core mesenchyme cells of the mandibular arch are both *Mesp1*- and *MyoD*-positive (arrowed); in contrast, mesodermal mesenchyme beneath the neural tube (Fig. 2B, white dotted line) is *Mesp1*-positive but *MyoD*-negative (asterisk).

In the chick ventral/anterior compartment of the head, non-endothelial components of blood vessels, i.e. pericytes and smooth muscle, are of neural crest origin (Etchevers et al., 2001). Patapoutian et al. (1995) reported that α-SMA is already present in developing embryonic muscles including the smooth muscle of blood vessel walls by E12.5. We therefore investigated the tissue origin of pericytes and vascular smooth muscle in the mainly neural crest-derived ventral/anterior compartment of the mouse head by double immunostaining for lacZ and alpha-smooth muscle actin (α-SMA) on sections of E12.5 heads from embryos of both genotypes (Fig. 4B–D or E–G). Consistent with the data from chick, lacZ localization did not overlap with α-SMA staining in the *Mesp1-cre/R26R* sections (Fig. 4B–D) but the two were co-localised in *Wnt1-cre/R26R* sections (Fig. 4E–G). These results suggest that in the craniofacial region of mouse embryos the endothelial cells of blood vessels are of mesodermal origin and the muscular components of the vessel walls are derived from neural crest.

2.5. *Mesodermal contribution to the skull vault and connective tissue*

As previously reported, X-gal staining of *Wnt1-cre/R26R* heads indicates that the neural crest-derived components of the skull vault are the frontal bone and the central part of the interparietal bone (Jiang et al., 2002); there is also a tongue

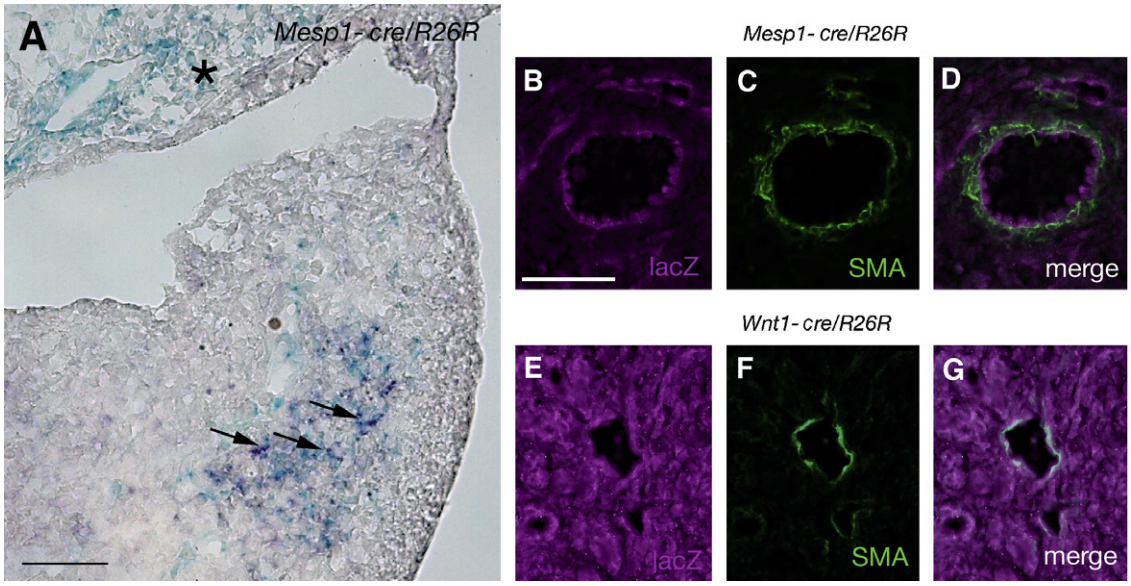

Fig. 4 – Myogenic lineage distribution. (A) X-gal staining (blue) and detection of *MyoD* transcripts (dark purple) on a horizontal section of the first branchial region of an E10.5 *Mesp1-cre/R26R* embryo; double-stained cells are present in the mandibular mesenchyme (arrows) but the mesenchyme above the pharynx (asterisk) is X-gal-positive only. (B–G) Double immunofluorescence detection of lacZ (magenta) and α -SMA (green) on the blood vessels in the first branchial region of E12.5 *Mesp1-cre/R26R* mice (B-D) and *Wnt1-cre/R26R* mice (E–G). (B–D) LacZ expression in endothelial cells (B) and immunoreactivity of α -SMA is present in the pericyte cell layer external to this (C,D). (E–G) Almost all mesenchymal cells around the blood vessel are lacZ-positive neural crest-derived cells (E), including the α -SMA-positive cells outlining the vessel (F,G); endothelial cells are unstained. Scale bars: A 200 μm; B–G 50 μm.

of neural crest-derived membrane between the two parietal bones (sagittal suture). We assumed that the parietal bones and the X-gal-negative part of the interparietal bone are mesodermal in origin. Comparison of the X-gal staining pattern of the skull vault at E17.5 in *Mesp1-cre/R26R* and *Wnt1-cre/R26R* fetuses (Fig. 5A and B) confirms this hypothesis.

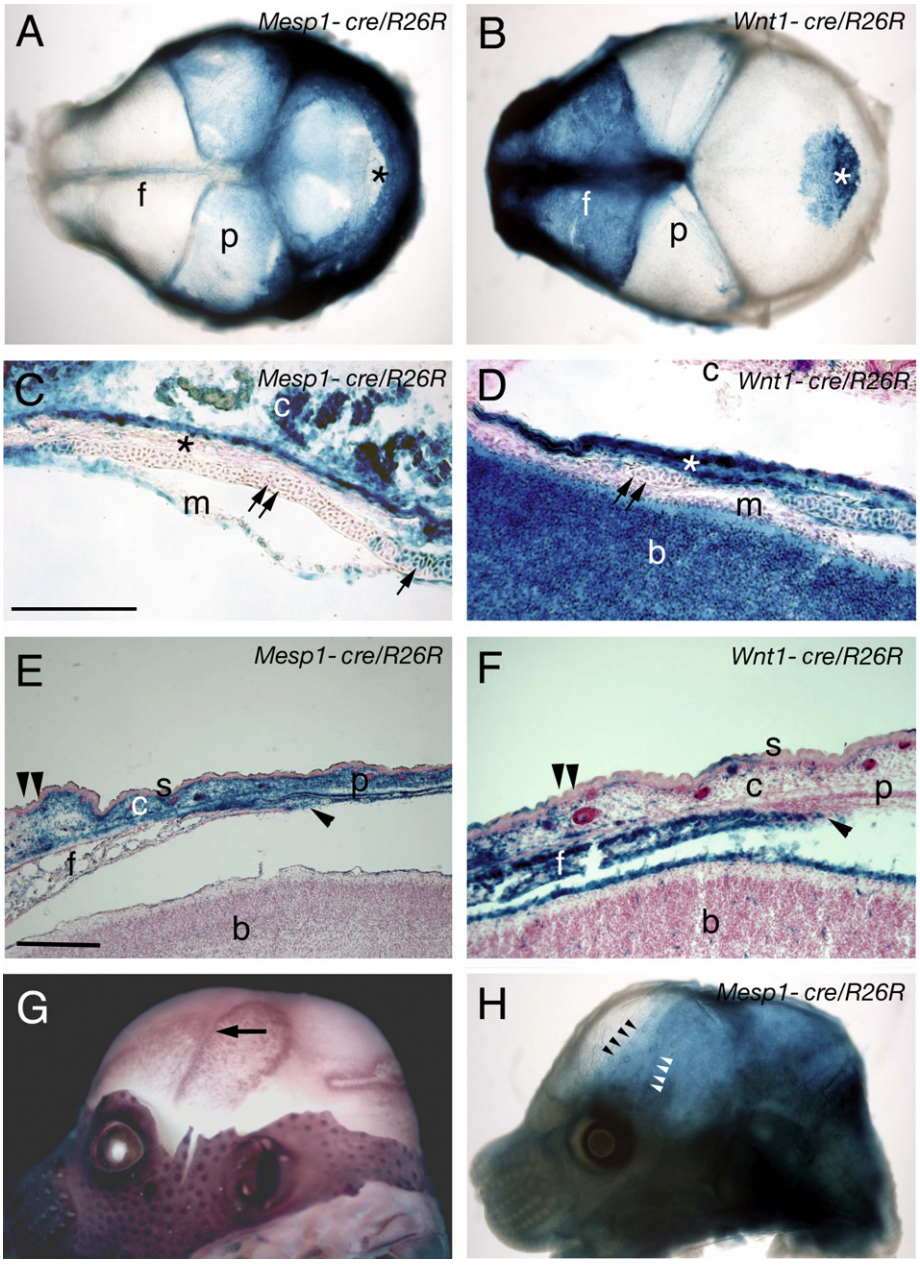

Fig. 5 – Tissue boundaries in the skull and adjacent mesenchyme. (A, B) Whole mount X-gal staining of skull vaults at E17.5, brain and the skin removed: reciprocal staining patterns are present in *Wnt1-cre/R26R* and *Mesp1-cre/R26R* skulls. (A) The parietal (p) and the lateral parts of the interparietal (asterisk) bones are of mesodermal origin; mesoderm-derived meninges underlie the interparietal bone, showing as a light blue-stained area (asterisk). (B) The frontal (f) bones and medial part of the interparietal bone (asterisk) are of neural crest origin; faint X-gal staining of the parietal bone is due to underlying neural crest-derived meninges. (C, D) X-gal staining of mid-sagittal sections of part of the interparietal bone showing reciprocal positive/negative staining patterns in the bone (asterisk), the underlying cartilage (double arrows) and meninges (m); part of the cartilage (arrow) appears to be composed of a mixed population. (E, F) Reciprocal patterns of X-gal staining of horizontal sections of the coronal suture (arrowhead) flanked by frontal (f) and parietal (p) bones: the neural crest-mesoderm boundary (double arrowheads) in the dermal connective tissue layer (c) is rostral to that of the skeletogenic layer. (G) Whole mount in situ hybridization of *Fgfr2* on an E15.5 head, skin partially removed; the coronal suture is arrowed. (H) X-gal staining of a halved E15.5 *Mesp1-cre/R26R* head, brain removed: the position of the coronal suture is marked by white arrowheads and the neural crest-mesoderm boundary in the dermal mesenchyme by black arrowheads. b, brain. Scale bars: C, D 200 μm; E, F 200 μm.

The two patterns are complementary and mutually exclusive, with neural crest-mesoderm boundaries at the coronal and sagittal sutures as previously reported. Faint X-gal staining in the frontal bone area of the *Mesp1-cre/R26R* skull represents blood vessels, and faint staining in the parietal bone area of the *Wnt1-cre/R26R* skull is due to the underlying neural crest-derived meningeal layer (Fig. 5A and B and Jiang et al., 2002). Since the meningeal covering of the midbrain is of mesodermal origin, faint X-gal staining is also seen through the medial X-gal-negative part of the interparietal bone in *Mesp1-cre/R26R* skulls (Fig. 5A, asterisk). X-gal staining of mid-sagittal sections showed complementary localization of LacZ expression indicating the presence of both neural crest and mesoderm in the interparietal bone and adjacent tissues (Fig. 5C and D).

The coronal suture comprises overlapping edges of the frontal and parietal bones; the sutural mesenchyme between them is mesodermal in origin (Fig. 5E and F). We previously demonstrated, but did not point out, that the dermal connective tissue overlying this suture is X-gal-negative in *Wnt1-cre/R26R* embryos (Jiang et al., 2002, Fig. 1E). Here we show that the neural crest-mesoderm boundary in this tissue lies rostral to the coronal suture (Fig. 5E and F), and that this positional discrepancy is present at an early stage of upgrowth of the frontal and parietal bones (Fig. 5G and H).

2.6. *Frontal and parietal bones grow over the meningeal layer by expanding their original primordia*

The frontal and parietal bone primordia appear in the baso-lateral region of the head and subsequently grow up towards the apex (Iseki et al., 1997; Rice et al., 2000). The early primordia express *Runx2* and are actively proliferating (Rice et al., 2003). During their expansion, the bones thicken, and the frontal bone develops a trabecular structure. Since the neural crest-mesoderm boundary between the up-growing bones is out of register with the boundary in the dermal connective tissue, it seemed unlikely that bone growth involved recruitment of cells from that layer. Although a previous study showed that some of the labeled frontal bone primordial osteogenic cells are localised in the apical region of the frontal bone after expansion (Yoshida, 2005), two possibilities remained: (1) that cells are recruited to the up-growing bones from a deeper connective tissue layer associated with the meninges; (2) that the bones are entirely or mainly formed by proliferation within, and expansion of, the original basolateral primordia. To distinguish between these two possibilities we undertook a series of experiments in which the bone primordia were labeled with the fluorescent dye, DiI, using ex-utero surgery. *Fgfr2* gene expression in whole heads reveals the position of the differentiating bone domains (Iseki et al., 1997). We therefore compared the pattern of *Fgfr2* expression at a series of stages to determine the optimum time for injecting the dye. The frontal and parietal domains and the future coronal suture between them are clearly visible at E13.5 (Fig. 6A). The most rapid period of growth takes place between E14.5 and E16.5 (not shown). We therefore chose E13.5 as the time of DiI injection, since the primordia are just starting to grow upwards but have not yet entered their most rapid growth phase.

In the first series of experiments, DiI was injected into the frontal primordium mesenchyme just above the superciliary ridge region (Fig. 6B); consistent with the previous result (Yoshida, 2005) the coronal section (Fig. 6C) shows that the frontal bone primordium region is labeled. After closure of the maternal abdomen, each fetus was allowed to develop for a further 96 or 120 h (E17.5 or E18.5, $n = 12$). After 120 h, the DiI-labeled area had expanded to fill the whole frontal bone domain (Fig. 6D). In coronal sections, labeled cells were detected throughout the frontal bone from base to apex (Fig. 6E); some connective tissue cells close to the injection site were also labeled, but at higher levels the labeling was entirely within the bone, sometimes very close to the interfrontal suture (Fig. 6F).

Next, we labeled the mesenchyme of E13.5 heads at a higher level, lateral to or in the midline, above the level of the bone primordia. When the mesenchyme just lateral to the midline was labeled (Fig. 6G, $n = 11$) and the fetuses examined 120 h later, the fluorescence was detected mainly in the meningeal

Fig. 6 – DiI labelling of the skull bone primordia and cranial mesenchyme. Fluorescent and bright field images are merged in B-L. (A) *Fgfr2* expression in an E13.5 whole head: frontal (f) and parietal (p) bone primordia are located at the basolateral side of the head, above the eye (e) and immediately caudal to this, respectively. (B–F) DiI labelling of the frontal bone primordium. (B) Lateral view of an E13.5 head just after labelling of the frontal bone primordium at the superciliary ridge. (C) Coronal section of (B) just after the injection, indicating that the dye strictly localizes at the injection site (white arrow). (D) Lateral view of a whole head 96 hours after labelling (E17.5). (E) Coronal section of a head collected 120 h after labeling: injected dye is in the developing frontal bone (f) and extends almost to the top of the head (white arrowhead). Some fluorescent cells are present in mesenchyme at the injection site (white arrow). (F) An example of a labelled cell at the very tip of the developing bone on a coronal section (white arrowhead) close to the interfrontal suture (is). (G–I) DiI labelling of the mesenchyme lateral to the midline (G, H) or in the midline (I). (G) Lateral view of an E13.5 head just after injection of DiI. (H) Coronal section of a fetal head 120 h after injection: fluorescence is present in the meningeal layer (m) between the developing frontal bone (f) and the brain (br). (I) Coronal section of a fetal head 96 h after the injection: fluorescence is present mainly in the midline tissue, the future interfrontal suture (is) and meningeal layer (arrows). The arrowhead indicates osteoid of the frontal bone. (J–N) DiI labelling of the parietal bone primordium. (J) Lateral view of a head just after injection of DiI. (K) 96 h after injection. (L) Coronal section 120 h after injection: fluorescence is present in the developing parietal bone (p). (M, N) Dark and bright field images of the area boxed in L: fluorescence is present within the parietal domain as far as the apex (white arrowhead). c, connective tissue; s, skin; ss, sagittal suture. Scale bars: C, E, I, L 200 μm; F, H, M, N 100 μm.

layer (Fig. 6H), and sometimes in the dermal connective tissue layer (data not shown), but never in the osteogenic layer. Labeling of the midline mesenchyme ($n = 2$) resulted in most of the labeled cells remaining in the midline, where they were mainly located in the meningeal layers around the sagittal sinus; a few were in the connective tissue layer, but none were detected in the bone-forming layer (Fig. 6I).

We similarly examined the growth pattern of the parietal bone by labeling the mesenchymal parietal primordium on E13.5 (Fig. 6J, $n = 4$). 96 h later the labeled area had expanded and extended vertically (Fig. 6K). The coronal section shows that the labeled cells were located in the upper two-thirds of the parietal bone, including its apical edge (Fig. 6L–N).

3. Discussion

3.1. *The Mesp1-cre/R26R mouse as a tool for mesoderm lineage studies*

We have here validated the *Mesp1-cre/R26R* mouse as a tool for defining the contribution of cells of the mesodermal lineage to mouse craniofacial development. Our observations confirm the validity of the conclusions we made previously concerning the mesodermal origin of X-gal-negative cells in the skull of *Wnt1-cre/R26R* embryos (Jiang et al., 2002), demonstrating the mesodermal origin of the parietal bone and confirming the coronal (fronto-parietal) suture as a neural crest-

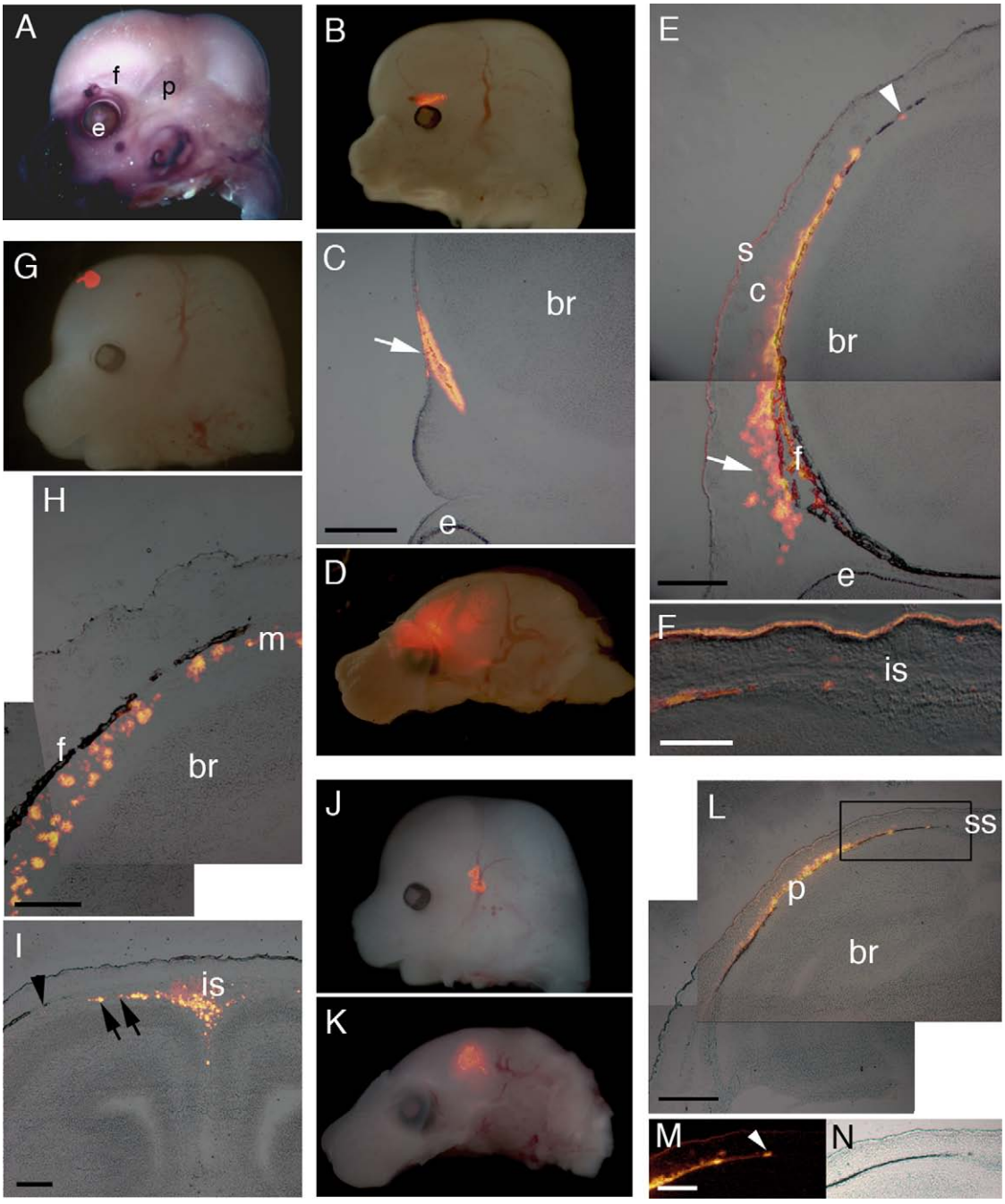

mesoderm boundary. Further, the availability of permanent markers for both neural crest and mesoderm has enabled parallel study of the development of these two tissues in combination with tissue-specific differentiation markers for cells of the endothelial and myogenic lineages.

3.2. *Integration of angioblasts and myoblasts within neural crest-derived mesenchyme*

The origin of endothelial cells in mouse embryos has previously been studied by whole mount immunolabelling using antibodies to several different epitopes (Drake and Fleming, 2000): Flk1 and TAL1 were found to identify angioblasts at the earliest stages, the first angioblasts being located in the extra-embryonic mesoderm at E6.3, and the first intra-embryonic angioblasts at E7.0, in the primordia of the endocardium. Blood vessels form within a day of the immunological detection of angioblasts at each site. By the 5- to 6-somite stage, (E8.3 of Drake and Fleming, 2000; E8.5 in our Figs. 1A–D and 3A and B) Flk1 immunostaining is distributed throughout the cranial mesenchyme. Our results confirm this observation and additionally show that angioblasts are the only cells of mesodermal origin so far identified that move into the stream of migrating neural crest cells, apparently as soon as the neural crest cells have formed as a mesenchymal population lateral and rostral to the mesodermal mesenchyme. This early incursion of mesodermal angioblasts into an apparently otherwise pure neural crest cell population enables blood vessels to form equally quickly within the neural crest-derived and mesoderm-derived mesenchyme of the head. Using *CD34* in situ hybridization, Wood et al. (1997) observed that condensing capillary networks can be seen in the head as early as the 14-somite stage, in a pattern that respects the anatomy of the developing non-vascular structures, e.g. eye and brain, with no reference to the boundary between what we now know to be two mesenchymal tissue domains. This can also be seen in at E10.5 embryo in our Fig. 3.

A rapid and pervasive invasiveness of angioblasts through cranial mesenchyme was demonstrated by Noden (1990), by transplanting early quail mesoderm into chick embryos and subsequently applying a quail endothelial cell-specific antibody on sections: quail angioblasts were found to be widely distributed within the chick mesenchyme, at surprising distances from the graft site. By combining mesenchymal markers for neural crest (*Wnt1-cre/R26R*) or mesoderm (*Mesp1-cre/R26R*) with Flk1 immunostaining, we have shown here that the movement of angioblasts from mesodermal to predominantly neural crest-derived mesenchymal domains can be detected without the need for transplantation. Even without immunostaining, the only X-gal-positive cells rostral to the major cranial boundary in the head of the *Mesp1-cre/R26R* embryos illustrated in Fig. 2B, M can be seen to resemble capillaries. Our results suggest that the mesodermal contribution to frontonasal mesenchyme detected by Trainor et al. (1994) in their mesodermal transplantation study most likely represents infiltration of the neural crest by angioblasts.

In contrast to angioblasts, cells of the myogenic lineage that migrate into the branchial arches remain within or close to their axial level of origin (Trainor et al., 1994; Noden and Trainor, 2005, and references therein). Our results confirm that the mesodermal cells that migrate as a discrete group into the core mesenchyme of the branchial arches are *MyoD*-positive. In contrast, the muscle cells (pericytes) that differentiate around blood vessels within the neural crest-derived craniofacial mesenchyme are of neural crest origin, indicating that formation of vessel myogenic components does not require mesodermal cell migration. These are expected results (Le Lièvre and Le Douarin, 1975; Etchevers et al., 2001), and make an important contribution to validating the *Mesp1-cre/R26R* mouse as a model organism for mesodermal lineage identification.

3.3. *Tissue origin of the skull vault*

Our previous study (Jiang et al., 2002) using *Wnt1-cre/R26R* embryos clearly showed that the neural crest-mesoderm boundary in the skull vault lies between the frontal and parietal bones. This observation has been generally accepted, but Matsuoka et al. (2005) illustrate a P0 X-gal-stained whole skull with a dotted line indicating the frontoparietal suture a short distance rostral to the *Wnt1*-positive boundary; they failed to recognize that the suture is formed as an overlap between the frontal and parietal bones and that while their line correctly identifies the border of the parietal bone, the border of the frontal bone lies at the boundary of the stained area (this observation requires the material to be sectioned). The tissue origins of the avian skull are more controversial, following the influential claim by Couly et al. (1993) that the whole avian skull vault is neural crest-derived. By means of targeted infection of *LacZ*-labeled retroviruses, Evans and Noden (2006) confirmed the earlier results of Noden (1978) and Le Lièvre (1978) that the neural crest-mesoderm boundary of the chick calvaria lies level with the caudal edge of the eye. A dual origin for the avian frontal bone is now accepted by several authors, who consider that it represents a fronto-parietal bone, the avian “parietals” being homologous with the post-parietals of reptiles and the interparietal of mammals (Jiang et al., 2002; Noden and Trainor, 2005; Hanken and Gross, 2005). Hanken and Gross (2005) further suggest that the “fronto-parietal” of anurans may be homologous with the frontal bone of other tetrapods, including mammals. With the exception of the avian study of Couly et al. (1993), all species in which mapping studies have been carried out place the caudal edge of the neural crest-derived part of the skull vault at the caudal edge of the orbit, providing a consistency that is more reliable than the terminology-based cross-species homologies derived from long-established adult skeletal anatomy nomenclature.

3.4. *A new mechanism for the growth of calvarial bones*

It is clear from observation of the developing mouse skull that the calvarial bones grow upwards towards the vertex of the skull from an initially basolateral position (Iseki et al., 1997). This pattern of upgrowth can also be seen in alizarin red preparations of the developing human skull (personal observations). Rice et al. (2003) showed that the early primordia express *Runx2*. Here we have shown by DiI-labelling of ex-utero embryos that in the mouse fetal head, the initially basolaterally-situated calvarial bone primordia grow vertically to form a layer of bone between the pre-existing dermal and meningeal

mesenchymal layers. The upward extension process involves expansion of the original *Runx2/Fgfr2*-expressing domains mainly or entirely by vertically-directed growth, without detectable recruitment of adjacent mesenchymal cells. This pattern of growth by primordium expansion is consistent with the growth of many other developing systems, especially epithelia such as the lungs (Minoo et al., 1999; for further examples and references, see Davies, 2005). Independence of the skeletal and dermal mesenchymal layers is further supported by our observation that the juxtaposed edges of the frontal and parietal bones, i.e. the calvarial neural crest-mesoderm boundary at the coronal suture, progressively lose alignment with the pre-existing dermal mesenchymal boundary as they extend upwards, so that by later stages of bone upgrowth the upper part of the suture lies caudal to the mesenchymal boundary.

The skull growth pattern we have elucidated here is fundamentally different from previous accounts of skull development that begin with formation of the meninx primitiva, a layer of mesenchyme surrounding the early embryonic brain, which splits into endomeninx and ectomeninx, the latter splitting again to form the bone-forming layer and dura mater (Sperber, 2001; Meikle, 2002 and references therein). According to that account, the frontal and parietal bones originate as ossification centers in their final positions, growing radially to form the radially-organized mineralization pattern that is clear in alizarinred-stained and dried human fetal skulls. Our observations suggest that in the mouse, and presumably in all mammals, the radial pattern of mineralization does not begin until after upgrowth of the bone domains is complete, by which stage the mineralized bones are miniatures of their adult forms and continuing growth involves a signalling system leading to progressive osteogenesis at the sutural margins (Iseki et al., 1999). This is an important distinction, since measurements between the centres of radial growth have been used to predict the developmental stage of origin of abnormal calvarial growth in craniosynostosis (Mathijssen et al., 1999).

The observation that calvarial bones and dermal mesenchyme develop independently renders inappropriate the term “dermal bone” as an alternative to “membrane bone” to describe the calvarial bones. Although our results cannot be extrapolated to interpretation of the developmental origin of the calvaria of other species, let alone membrane bones in other sites, it is interesting to note that the plastron of turtles, previously described as dermal bone (de Beer, 1951), is derived from neural crest and does not form in situ within the dermis (Cebra-Thomas et al., 2007). Further studies may reveal that other membrane bones are independent of the dermis in their origins.

4. Materials and methods

4.1. *Animals*

All transgenic mouse lines, i.e. *Mesp1-cre*, *Wnt1-cre*, and the *R26R* conditional reporter allele have been described previously (Chai et al., 2000; Saga et al., 1996; Soriano, 1999). C57BL/6 mice were used as wild type mice for immunohistochemistry and ex-utero surgery. The morning that the vaginal plug was identified was designated as embryonic day 0.5 (E0.5). All animal experiments were carried out in accordance with protocols certified by the Institutional Animal Care and Use Committee of Tokyo Medical and Dental University and National Institute of Genetics. All efforts were made to minimize the number of animals used and their suffering.

4.2. *Methods for X-gal staining, in situ hybridization and immunohistochemistry*

X-gal staining was carried out on fresh or fixed frozen sections or whole mount specimens for early stages. Whole mount specimens were then embedded into paraffin and sectioned. Counter-staining was carried out with eosin or nuclear red. Mouse *Fgfr2* (1.96 kb of IgIIIa/IIIc splice variant, including the whole extracellular and transmembrane domains) and mouse *MyoD* (MluI and SphI fragment of 967b) were used for in situ hybridization (ISH). To generate antisense and sense transcripts, the plasmids were linearized and transcribed using T3 or T7 RNA polymerase. All transcripts were reduced to an average size of 250 bases by limited alkaline hydrolysis. ISH was carried out on fresh frozen sections, 4% paraformaldehyde (PFA)/PBS fixed frozen sections and on whole head samples as described by Iseki et al. (1997).

Immunohistochemical detection of lacZ, Flk1, CD31 (PECAM) was carried out on 4% PFA/PBS fixed frozen sections or whole mount specimens by using rabbit anti-lacZ (Cappel), rat anti-Flk1 (BD Pharmingen) and/or rat anti-CD31 (BD Pharmingen) antibodies. For sections, visualization was carried out by means of secondary antibodies labelled with alexa fluor 488 or 555 (Invitrogen); for whole mount specimens, specific binding of horse radish peroxidase-labelled secondary antibody was detected by the 3,3′-diaminobenzidine colour reaction.

2.3. *DiI label tracing in ex-utero embryos*

Skull vault growth was investigated by injection of DiI (1,1′-dioctadecyl-3,3,3′,3′-tetramethyl-indocarbocyanine perchlorate; Invitrogen, USA), prepared by dilution of a saturated DiI solution in *N*,*N*-dimethylformamide in 0.3 M sucrose at 1:30. Injection of DiI into specific sites in the E13.5 mouse fetal head was carried out by ex-utero surgery (Iseki et al., 1997) and the pregnancy was allowed to continue for 96 h (E17.5) or 120 h (E18.5).

Acknowledgement

We are grateful to J. Heath (*Fgfr2*) and M. Buckingham (*MyoD*)-for providing with the plasmids and K. Morinaka for her technical support. This work was supported by Grants in Aid for Scientific Research From the Japanese Ministry of Education, Culture, Sports, Science and Technology (No. 15390554) and a funding by NIG Cooperatice Research Program (2005-A33).

REFERENCES

Chai, Y., Jiang, X., Ito, Y., Bringas Jr., P., Han, J., Rowitch, D.H., Soriano, P., McMahon, A.P., Sucov, H.M., 2000. Fate of the

mammalian cranial neural during tooth and mandibular morphogenesis. Development 127, 1671–1679.
Chan, W.Y., Tam, P.P.L., 1988. A morphological and experimental study of the mesencephalic neural crest cells in the mouse embryo using wheat germ agglutinin-gold conjugate as the cell marker. Development 102, 427–442.
Cebra-Thomas, J.A., Betters, E., Yin, M., Plafkin, C., McDow, K., Gilbert, S.F., 2007. Evidence that a late-emerging population of trunk neural crest cells forms the plastron bones in the turtle Trachemys scripta. Evol. Dev. 9, 267–277.
Couly, G.F., Coltey, P.M., Le Douarin, N.M., 1993. The triple origin of skull in higher vertebrates: a study in quail-chick chimeras. Development 117, 409–429.
Danielian, P.S., Maccino, D., Rowitch, D.H., Michael, S.K., McMahon, A.P., 1998. Modification of gene activity in mouse embryos in utero by a tamoxifen-inducible form of Cre recombinase. Curr. Biol. 8, 1323–1326.
Davies, J., 2005. Mechanisms of Morphogenesis: The Creation of Biological Form. Elsevier, London.
de Beer, G.R., 1951. Vertebrate Zoology. Sidgewick and Jackson Ltd., London.
Drake, C.J., Fleming, P.A., 2000. Vasculogenesis in the day 6.5–9.5 mouse embryo. Blood 95, 1671–1679.
Echelard, Y., Vassileva, G., McMahon, A.P., 1994. Cis-acting regulatory sequences governing Wnt-1 expression in the developing mouse CNS. Development 120, 2213–2224.
Etchevers, H.C., Vincent, C., Le Douarin, N.M., Couly, G.F., 2001. The cephalic neural crest provides pericytes and smooth muscle cells to all blood vessels of the face and forebrain. Development 128, 1059–1068.
Evans, D.J.R., Noden, D.M., 2006. Spatial relations between avian craniofacial neural crest and paraxial mesoderm cells. Dev. Dyn. 235, 1310–1325.
Hanken, J., Gross, J.B., 2005. Evolution of craniofacial development and the role of neural crest: insights from amphibians. J. Anat. 207, 437–446.
Iseki, S., Wilkie, A.O., Heath, J.K., Ishimaru, T., Eto, K., Morriss-Kay, G.M., 1997. Fgfr2 and osteopontin domains in the developing skull vault are mutually exclusive and can be altered by locally applied FGF2. Development 124, 3375–3384.
Iseki, S., Wilkie, A.O.M., Morriss-kay, G.M., 1999. Fgfr1 and Fgfr2 have distinct differentiation- and proliferation-related roles in the developing mouse skull vault. Development 126, 5611–5620.
Jiang, X., Rowitcch, D.H., Soriano, P., McMahon, A.P., Sucov, H.M., 2000. Fate of the mammalian cardiac neural crest. Development 127, 1607–1616.
Jiang, X., Iseki, S., Maxson, R.E., Sucov, H.M., Morriss-Kay, G.M., 2002. Tissue origins and interaction in the mammalian skull vault. Dev. Biol. 241, 106–116.
Le Douarin, N.M., Kalcheim, C., 1999. The Neural Crest. Cambridge University Press, Cambridge.
Le Lièvre, C.S., Le Douarin, N.M., 1975. Mesenchymal derivatives of the neural crest: analysis of chimeric quail and chick embryos. J. Embryol. Exp. Morphol. 34, 125–154.
Le Lièvre, C.S., 1978. Participation of neural crest-derived cells in the genesis of the skull in birds. J. Embryol. Exp. Morphol. 47, 17–37.
Mathijssen, I.M., van Splunder, J., Vermeij-Keers, C., Pieterman, H., de Jong, T.H., Mooney, M.P., Vaandrager, J.M., 1999. Tracing craniosynostosis to its developmental stage through bone center displacement. J. Craniofac. Genet. Dev. Biol. 19, 57–63.
Matsuoka, T., Ahlberg, P.E., Kessaris, N., Iannarelli, P., Dennehy, U., Richardson, W.D., McMahon, A.P., Koentges, G., 2005. Neural crest origins of the neck and shoulder. Nature 436, 347–355.
Meikle, M., 2002. Craniofacial Development. Growth and Evolution. Bateson Publishing, Norfolk, England.
Minoo, P., Su, G., Drum, H., Bringas, P., Kimura, S., 1999. Defects in tracheoesophageal and lung morphogenesis in Nkx2.1(−/−) mouse embryos. Dev. Biol. 209, 60–71.
Nichols, D.H., 1981. Neural crest formation in the head of the mouse embryo as observed using a new histological technique. J. Embyol. Exp. Morphol. 64, 105–120.
Noden, D.M., 1978. The control of avian cephalic neural crest cytodifferentiation. I. Skeletal and connective tissues. Dev. Biol. 67, 296–312.
Noden, D.M., 1990. Origins and assembly of avian embryonic blood vessels. Ann. NY Acad. Sci. 588, 236–249.
Noden, D.M., Trainor, P.A., 2005. Relations and interactions between cranial mesoderm and neural crest populations. J. Anat. 207, 575–601.
Osumi-Yamashita, N., Ninomiya, Y., Doi, H., Eto, K., 1994. The contribution of both forebrain and midbrain crest cells to the mesenchyme in the frontonasal mass of mouse embryos. Dev. Biol. 164, 409–419.
Parr, B.A., Shea, M.J., Vassileva, G., McMahon, A.P., 1993. Mouse *Wnt* genes exhibit discrete domains of expression in the early embryonic CNS and limb buds. Development 119, 247–261.
Patapoutian, A., Wold, B.J., Wagner, R.A., 1995. Evidence for developmentally programmed transdifferentiation in mouse esophageal muscle. Science 270, 1818–1821.
Rice, D.P.C., Aberg, T., Chan, Y.S., Tang, Z., Kettunen, P.J., Pakarinen, L., Maxson, R.E., Thesleff, I., 2000. Integration of FGF and TWIST in calvarial bone and suture development. Development 127, 1845–1855.
Rice, R., Rice, D.P., Olsen, B.R., Thesleff, I., 2003. Progression of calvarial bone development requires Foxc1 regulation of Msx2 and Alx4. Dev. Biol. 262, 45–87.
Saga, Y., Hata, N., Kobayashi, S., Magnuson, T., Seldin, M.F., Taketo, M.M., 1996. MesP1: a novel basic helix-loop-helix protein expressed in the nascent mesodermal cells during mouse gastrulation. Development 122, 2760–2778.
Saga, Y., Miyagawa-Tomita, S., Takagi, A., Kitajima, S., Miyazaki, J., Inoue, T., 1999. Mesp1 is expressed in the heart precursor cells and required for the formation of a single heart tube. Development 126, 3437–3447.
Sakai, K., Miyazaki, J., 1997. A transgenic mouse line that retains Cre recombinase activity in matuture oocytes irrespective of the cre transgene transmission. Biochem. Biophys. Res. Commun. 237, 318–324.
Serbedzidja, G.N., Bronner-Fraser, M., Fraser, S.E., 1992. Vital dye analysis of cranial neural crest cell migration in the mouse embryo. Development 116, 297–307.
Soriano, P., 1999. Generalized lacZ expression with the ROSA26 Cre reporter strain. Nat. Genet. 21, 70–71.
Sperber, G., 2001. Craniofacial Development. BC Decker Inc., Hamilton, Canada.
Tan, S.S., Morriss-Kay, G.M., 1986. Analysis of cranial neural crest cell migration and early fates in postimplantation rat chimaeras. J. Embyol. Exp. Morphol. 98, 21–58.
Trainor, P.A., Tan, S.S., Tam, P.P.L., 1994. Cranial paraxial mesoderm: regionalization of cell fate and impact on craniofacial development in mouse embryos. Development 120, 2397–2408.
Trainor, P.A., Tam, P.P.L., 1995. Cranial paraxial mesoderm and neural crest cells of the mouse embryo: co-distribution in the craniofacial mesenchyme but distinct segregation in branchial arches. Development 121, 2569–2582.
Yoshida, T., 2005. Growth pattern of the frontal bone primordium and involvement of Bmps in this process. Kokubyo Gakkai Zasshi 72, 19–27.
Wood, H.B., May, G., Healy, L., Enver, T., Morriss-Kay, G.M., 1997. CD34 expression patterns during early mouse development are related to modes of blood vessel formation and reveal additional sites of haematopoiesis. Blood 90, 2300–2311.